Palm-Sized Laser Spectrometer with High Robustness and Sensitivity for Trace Gas Detection Using a Novel Double-Layer Toroidal Cell

Shiling Feng, Xuanbing Qiu, Guqing Guo, Enhua Zhang, Qiusheng He, Xiaohu He, Weiguang Ma, Christa Fittschen, Chuanliang Li

A palm-sized laser spectrometer with high robustness and sensitivity for trace gas detection using a novel double-layer toroidal cell

Shiling Feng[a], Xuanbing Qiu[a], Guqing Guo[a], Enhua Zhang[a], Qiusheng He[a], Xiaohu He[a], Weiguang Ma[b], Christa Fittschen[c], Chuanliang Li[a,*]

[a]*School of Applied Science, Taiyuan University of Science and Technology, Taiyuan 030024, China*

[b]*State Key Laboratory of Quantum Optics and Quantum Optics Devices, Institute of Laser Spectroscopy, Shanxi University, Taiyuan 030006, China*

[c]*Université Lille, CNRS, UMR 8522 - PC2A - Physicochimie des Processus de Combustion et de l'Atmosphère, Lille F-59000, France*

[*]*Corresponding author: li_chuanliang@126.com*

Abstract: A palm-sized laser spectrometer has been developed for detecting trace gases based on tunable diode laser absorption spectroscopy (TDLAS) in combination with a novel double-layer toroidal cell. With the benefit of a home-made electronic system and compact optical design, the physical dimension of the sensor is minimized into 24×15×16 cm^3. A toroidal absorption cell, with 84 reflections in 2 layers for an effective optical path length of 8.35 m, was used to enhance the absorption signals of gaseous species. A home-made electronic system was designed for implementing distributed feedback (DFB) diode laser controller, analog lock-in amplifier, data acquisition and communication. Calibration-free scanned wavelength modulation spectroscopy was employed to determine the concentration of the gas and reduce the random fluctuations from electronical noise and mechanical vibration. The measurement of CH_4 in ambient air was demonstrated using a DFB laser at 1.653 μm. The rise time and fall time for renewing the gas mixture are approximately 16 s and 14 s, respectively. Vibration and temperature tests have been carried out for verifying the performance of the spectrometer, and standard deviations of 0.38 ppm and 0.11 ppm for 20 ppm CH_4 at different vibration frequencies and temperatures, respectively, have been determined. According to the Allan deviation analysis, the minimum detection limit for CH_4 can reach 22 ppb at an integration time of 57.8 s. Continuous measurement of atmospheric CH_4 for two days validated the feasibility and robustness of our laser spectrometer, providing a promising laser spectral sensor for deploying in unmanned aerial vehicles or mobile robots.

Key words: palm-sized laser spectrometer, double-layer toroidal cell, near infrared spectroscopy, calibration-free scanned WMS, vibration and temperature environment tests

Introduction

Trace gas detection plays an important role in multiple application fields, such as analyzing human breath[1], monitoring pollutants[2] or greenhouse gases[3] and measuring gases of interest in industrial process[4]. A variety of conventional techniques are successfully used for trace gas detection, such as gas chromatography[5], mass spectroscopy[6] and Fourier transform spectroscopy[7]. Although these methods have high sensitivity and selectivity, they are costly, time-consuming and bulky. Therefore, these approaches are not suitable for a *real-time, in-situ* and mobile measurement of trace gases. Tunable diode laser absorption spectroscopy (TDLAS) has been widely employed in detecting trace gases due to its high selectivity, sensitivity and rapid response[8-11]. In recent years, the trend of compact laser spectrometers has been the focus of TDLAS for fulfilling the embedding requirements for unmanned aerial vehicles[12] or mobile robots[13]. Due to restriction of physical dimension, the effective optical path length is commonly shortened, which decreases the detection sensitivity of the sensor. Therefore, a multipass cell (MPC) is a better choice for compact laser spectrometer. White cells[14, 15], Herriott cells[16-18] and Chernin absorption cells[19] are three typical MPC used in TDLAS. These absorption cells consist of two or more individual mirrors. However, they are susceptible to mechanical vibration and temperature variation. Thus, a compact, stable and well-adapted absorption cell is desirable for a TDLAS senor to be employed in artificial intelligence inspection vehicles. Recently, a compact toroidal MPC with low-volume monolithic ring[20, 21] was presented and we also proposed a toroidal cell with multi-layer patterns[22].

Wavelength modulation spectroscopy (WMS)[17, 23], offering a substantial decrease of 1/*f* noise, is a preferred technique in TDLAS to improve the sensitivity and robustness via transforming the detection frequency to a higher region. In contrast to direct absorption spectroscopy, the absolute concentration of a targeted gas cannot be determined from WMS spectral signals: the intensity of the WMS signal is dependent on pressure, temperature and laser output power *etc*. In order to lessen the common-mode noise, Rieker *et al*. proposed the 2*f*/1*f* normalization[24], and Wang *et al*. developed a 2*f*/DS-sine to further simplify the calibration approach[25]. Moreover, Qu *et al.* presented a calibration-free scanned wavelength modulation spectrometer to derive species concentration and temperature by fitting to the 2*f*/1*f*-WMS lineshapes[26]. The previous calibration-free WMS methods, in most cases, were based on a digital lock-in technique that demanded huge amounts of computing resources and was usually time-consuming. For the goal of fast response measurements, analog lock-in technology offers the function of instant demodulating process without occupying computing resources. Therefore, it is suitable for *real-time* WMS detection, especially

for some cases including complex spectral line fitting procedures.

CH_4 is of significant importance due to its strong greenhouse effect, and it's use in industry and urban utility, so its detection is critical for global warming and safety in human activity[27-29]. On-board compact laser sensors for patrol vehicles can enormously increase the efficiency of leakage inspection. The strong fingerprint fundamental bands for CH_4 locate at around 3.3 μm and 7.3 μm, so it is easy to reach sensitive detection in the corresponding regions. Based on the WMS, Qu *et al.* used mid-IR quantum cascaded laser (QCL) to detect CH_4 at 7.5 μm and achieved a sensitivity of 0.04 ppm[30]. Dong *et al.* monitored CH_4 by using a 3.3 μm interband cascade laser and achieved minimum detection limit of 1.4 ppb for a 60 s averaging time[31]. Nevertheless, mid-IR diode lasers and detectors are more expensive, bulky and less durable compared to robust near-IR diode lasers. Thus, near infrared diode lasers are more appropriate for integration into small-sized laser sensors. Recently, Liu *et al.*[32] and Dong *et al.*[33], respectively, developed the novel multi-pass cells with low-volume and achieved a minimum detection limit of tens to hundreds ppb in the near-IR region.

In this work, a palm-sized spectrometer was developed based on TDLAS combining with a novel double-layer toroidal absorption cell (DLTAC). A home-made electronic circuit system was designed for laser control, signal acquisition, demodulation and data communication. Calibration-free scanned (CFS)-WMS was employed and a lineshape fitting procedure was carried out for deriving the concentration of the trace gas. The measurement of CH_4 was performed by a distributed feedback (DFB) diode laser. The characteristics, such as response time and robustness towards temperature variation and mechanical vibration were measured for characterizing the performance of the spectral sensor. Allan deviation was utilized to analyze the stability of the sensor. To validate the application of the sensor, a demonstration of atmospheric CH_4 monitoring was shown by two days of continuous detection.

Principle of CFS-WMS

For WMS, both the laser intensity and laser wavelength (frequency) are modulated by a high frequency sinusoidal modulation (f_m) superposed in a low frequency sawtooth scan (f_s). For one sawtooth period, the expression of the wavelength $v(t)$ is described as[26]:

$$v(t) = v_s(t) + a(t)\cos(2\pi f_m t + \theta)\,, \tag{1}$$

where $v_s(t)$ is the center laser wavelength without modulation and $a(t)$ is the modulation depth that relies on the amplitude of the modulation signal, θ is the initial phase of wavelength modulation. According to Lambert-Beer's law, the laser intensity transmitted through the absorbing species is represented as:

$$I(t) = I_0(t)\exp[-\alpha(v)] = I_0(t)\exp[-cPLS(T)\varphi(v)], \tag{2}$$

where $I_0(t)$ is the laser intensity without absorbing medium and $\alpha(v)$ is the absorbance defined by the concentration of the detected gas c, total pressure P, optical length L. Herein, line strength of transition $S(T)$ relies on the temperature of the gas T in the cell and on the line shape function $\varphi(v)$. The harmonic signals S_{nf} are extracted by a lock-in amplifier:

$$S_{nf} = \sqrt{\left[I(t)\sin(2\pi n f_m t) \otimes LPF\right]^2 + \left[I(t)\cos(2\pi n f_m t) \otimes LPF\right]^2}, \tag{3}$$

where LPF is a low-pass filter. The WMS-2f signal is the preferred option relating with the signal to noise (SNR) and the signal amplitude at the center of the absorption line. The 2nd-harmonic signal normalized by the 1st-harmonic signal (WMS-2f/1f)[34] can improve the robustness and reliability of sensors in harsh environments. The concentration of the absorbing gas is determined by least-square fitting of the observed WMS-2f/1f signal to lineshape function. For reliable fitting, temperature and pressure were measured by built-in sensors.

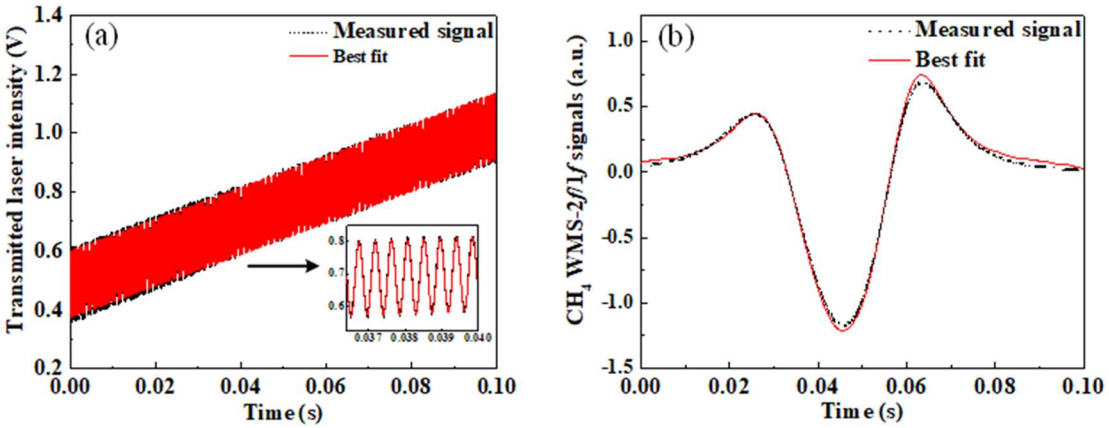

Fig.1 (a) Measured (black dash line) and fitted simulated (red solid line) transmitted laser intensity; (b) Measured (black dash line) and fitted simulated (red solid line) WMS-2f/1f signal of 40 ppm CH_4.

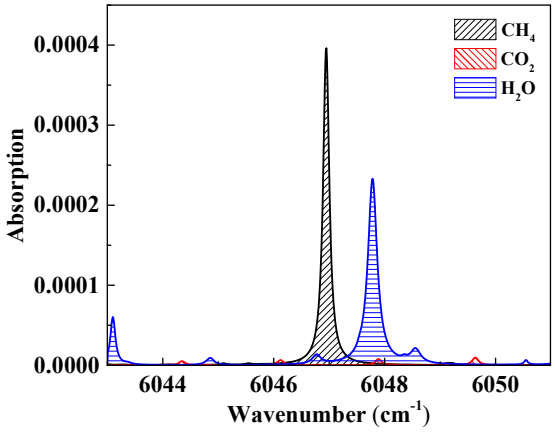

Fig. 2. Simulated spectra of CH_4 (3 ppm), CO_2 (400 ppb) and H_2O (1%) in the range of 6043-6051 cm^{-1} at 1atm with an optical path length of 8.4 m based on HITRAN.

The amplitude of WMS-2*f*/1*f* signal depends dramatically on both modulation amplitude (MA) and phase shift (PS) between laser intensity and wavelength modulation, therefore these factors need to be known before fitting WMS-2*f*/1*f* signal. In the present CFS-WMS scheme, MA and PS are determined by least-square fitting the direct absorption spectral signal to the measured signal in the presence of the absorbing gas, as depicted in Fig. 1(a). The temperature and pressure parameters in Eq.(2) can be obtained by built-in sensor. Then, the concentration was derived by fitting the observed WMS-2*f*/1*f* signal using a Lorentzian function[35], plotted in Fig. 1(b).

H_2O and CO_2 are two perturbing species to the CH_4 spectral measurement near 1.65 μm, so it is necessary to choose a discrete and strong CH_4 absorption line. Based on the HITRAN 2016 database[36], the absorption lines for 30 ppm CH_4, 1% H_2O and 0.3% CO_2 around 6047 cm^{-1} are simulated at 1 atm, 300 K and 8.4 m absorption path, and are plotted in Fig. 2. As depicted in Fig. 2, the CH_4 line is discret and the influence from H_2O can be neglected. To ensure that the H_2O concentration was less than 0.1% even for applications at high humidity, a drier was applied in our measurements.

Experimental

The schematic diagram of the palm-sized spectrometer for CH_4 is shown in Fig. 3(a). The output of a fiber-coupled distributed feedback (DFB) diode laser (NLK1U5FAAA, NEL) operated at 1.653 μm and room temperature passed through an optical collimator and was then coupled to a novel DLTAC. In principle, it is more suitable for ICL or QCL lasers emitting at the mid-infrared spectral region than the near infrared one due to our gold-coated inner surface with a higher reflectivity. The laser scanned from 6043 to 6050 cm^{-1}, covering the CH_4 line at 6046.96 cm^{-1}. The temperature of the TEC was fine-tuned around 25.1 ℃ for guaranteeing the absorption peak of CH_4 being located at the center of the scanning range. The output laser intensity from the DLTAC was collected by a home-made extended InGaAs detector (Netopto, NT52-1K-N). The thermometer and barometer sensors were used to monitor the parameters of the ambient atmosphere. As shown in Fig.3 (b), the physical dimension of the sensor is minimized into 24×15×16 cm^3 due to the compact optical and home-made electronic design. The sensor is made of aluminum alloy, a low dense material, while the thin toroidal multipass cell is made of stainless steel. The total weight of the sensor is 2.2 kg. The wavelength modulation and WMS-2*f*/1*f* signal were applied to enhance the detection sensitivity.

The effective optical path length of the DLTAC is 8.35 m with 84 reflections exhibiting a polygon star spot pattern of two layers. It was indicated that the optical interference was weak, and the signal amplitude was rational for our designed toroid cell at 8 meters optical path length. The laser entrance and exit angles are both 8.57°. The number of reflections is determined by both the angle of incidence and the curvature radius in sagittal plane (R_s) and tangential plane (R_t). Herein, R_t is 99.57 mm and R_s is 50 mm. For illustrating the practical beam pattern, a 650 nm laser was used to form the visible beam trace, as presented in the insert of Fig.3 (b).

The electronic part includes the temperature and current controller of the laser, the signal acquisition, temperature and pressure sensors, analog lock-in amplifier and data communication. The spectrometer is powered by business electricity with AC 220 V or by DC with 5 V for laser controller and 15 V for analog lock-in amplifier. The total electrical power consumption of the sensor is less than 10 W. The current sensor is powered by the homemade power board supplied by AC 220V, and it can also be powered by a battery. The laser controller module was designed on an 8 cm diameter PCB board. For the analog lock-in amplifier, the modulated signal at 7.572 kHz was generated by a voltage controlled oscillator (74HC4046A). A complex programmable logic device (CPLD, Altera, EPM7064AE) produced 1*f* and frequency-doubling (2*f*) signals and phase-shift. One of the 1*f* TTL signals

from the CPLD output was smoothed by a 5th order Butterworth low-pass filter and superposed with slow sawtooth signal at 5 Hz. The output of the photo detector was first acquired by the ADC for determining the parameters of the laser and then demodulated by two AD630 lock-in amplifiers for 1*f* and 2*f*. Two LPFs were used for further filtration, respectively. The demodulated signals were collected by the ADC (AD7616) and then transmitted to the microcontroller unit (STM32F405). ADC was used for fitting the 2*f*/1*f* spectral signal transmitted by a serial port. The concentration of the trace gas can be derived by a least-square fitting procedure.

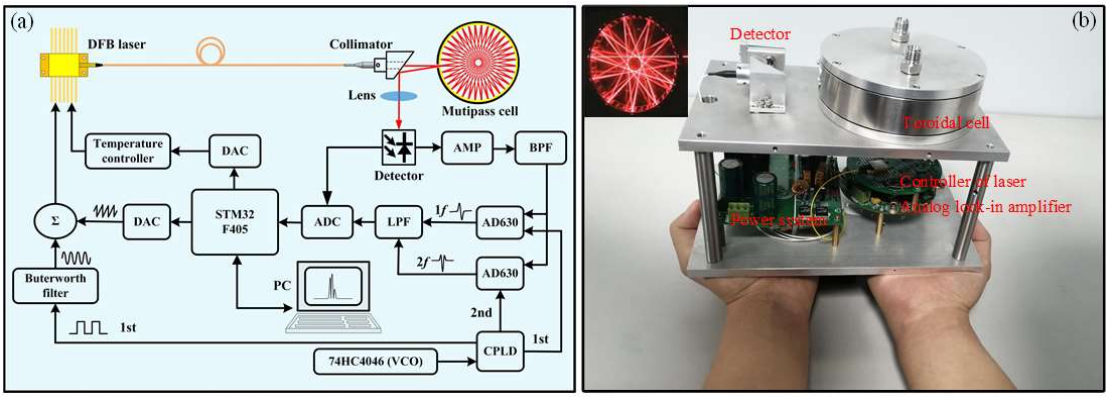

Fig. 3. (a) Schematic diagram of the experimental setup for CH_4 detecting; (b) photograph of the real instrument

Results and discussion

In wavelength modulation spectroscopy, the amplitude of the WMS-2*f*/1*f* signal depends on the modulation amplitude[32, 37]. To determine the optimum modulation amplitude, WMS-2*f* signals of 50 ppm CH_4 were measured at a series of modulation amplitudes at atmospheric pressure. From the measured signal, the maximum signal for CH_4 is obtained at 0.27 V and the corresponding modulation index is around 2.2[37, 38], which is in accordance with the theoretical prediction. Thus, a modulation amplitude of 0.27 V was employed in the following measurements. To verify the CFS-WMS principle, the measured and simulated WMS-2*f*/1*f* signals of a series of different CH_4 concentrations are presented in Figure 4: CH_4 concentrations in the range of 7 - 40 ppm were derived by diluting a calibrated gas mixture of 50 ppm CH_4 with pure N_2.

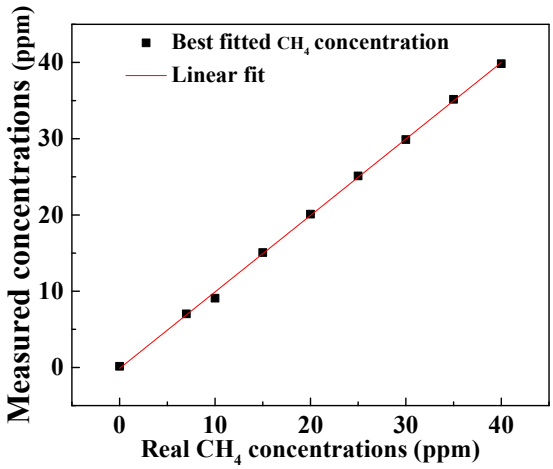

Fig. 4. Linear relationship between the real concentrations and the fitted ones.

Tests were performed to investigate the performance of our sensor to mechanical vibrations and changes in ambient temperature. The vibration test is a crucial index to evaluate an on-board or airborne sensor. The toroidal multipass cell is constructed by a monolithic ring, so its instinct is immune to vibration effect. The slight intensity fluctuation of laser is mainly arisen from a tiny displacement between the incident beam and the toroidal multipass cell due to mechanical vibration. As presented in Figure 5(a), the vibration test was simulated by a shaker table (Fang Ce Precision instrument technology co. LTD, LD-35BL) with frequency from 0 to 400 Hz. As shown in Fig.5(b), the concentration of the cell was set to 20 ppm. Overall, the difference between the measured and the real concentration was small in the entire range from 0 to 400 Hz. The largest error bar occurs at 200 Hz. It can be deduced that the natural frequency of our spectrometer is approximately 200 Hz. The test shows that the standard deviation of measurement is 0.36 ppm. The spectral intensity of peak-peak is sensitive to temperature variation, so

one needs to either keep the temperature constant or correct the temperature influence if the sample concentration is determined by the spectral peak-peak amplitude. As depicted in Fig.5(c), a test of our sensor to variation of the temperature is carried out by a high-low temperature test box (Wuxi yi'er da test equipment manufacturing Co., Ltd, GDW-150). The temperature interval was set to 10 ℃ and each temperature took 30 min to ensure the stability and reliability of the measurement. It illustrates that the peak-peak values of the spectra show an approximately linear decrease as the temperature increases from -10 to 50 ℃, as presented in Fig.5(d). However, the temperature influence is diminished by line-fitting considering the temperature factor. The standard error, as result of temperature variation, is approximatly 0.11 ppm from -10 to 50 ℃.

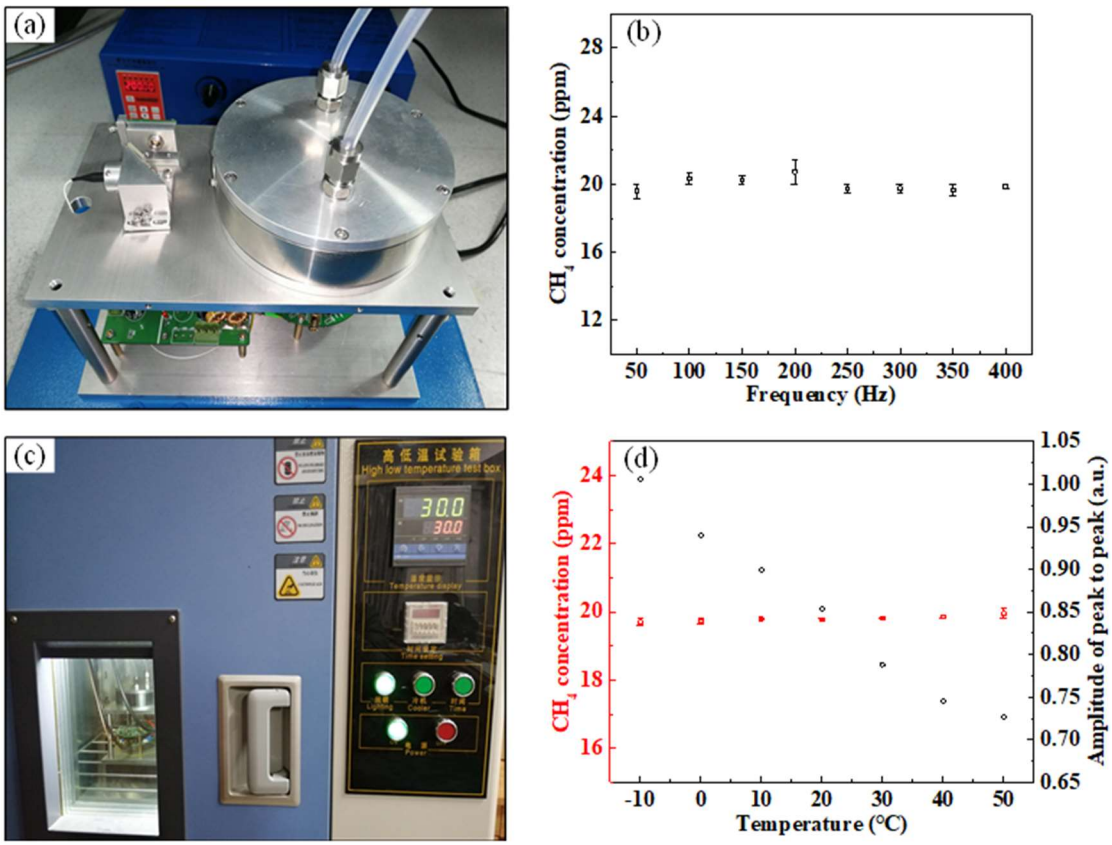

Fig.5 (a) Layout of the vibration test; (b) measured results obtained for 20 ppm CH_4 at different vibration frequencies; (c) structure of the temperature test; (d) observed amplitude of peak-peak of WMS-2*f*/1*f* and best fitted concentration of 20 ppm CH_4 at different temperatures.

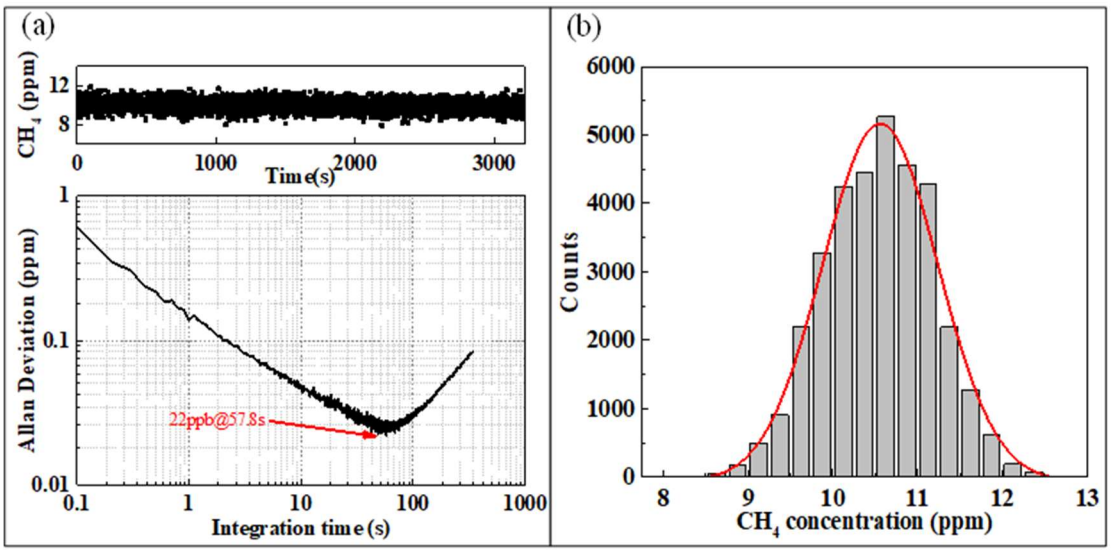

Fig.6. (a) Row data of individual concentration measurements over 400 s (top) and Allan variance as the function of integration time

(bottom); (b) histogram plot acquired from the time series measurement of 10 ppm CH_4. The red line is a Gaussian profile fitting.

To evaluate the detection precision and the stability of the sensor, the signal of 20 ppm CH_4 sealed in the cell was measured for about one hour. 34320 data points were obtained with the scan frequency of 5 Hz. As shown in Fig. 6(a), the Allan variance is a function of the measurement time. The figure indicates that the minimum detection limit is reached at 57.8 s and the minimum detectable concentration can be down to 22 ppb. The histogram of the measured concentration of CH_4, helpful to evaluate the measurement precision, is plotted in Fig. 6(b). The data distribution resembles a Gaussian profile, red line in Fig. 6(b). The measurement precision, determined by the half width at half maximum (HWHM), was found to be 0.8 ppm and the R^2 value and the standard deviation value (σ) were calculated to be 0.986 and 0.680 ppm, respectively. The high sensitivity and high measurement precision confirm the high performance of the developed CH_4 sensor based on toroidal multipass cell. The dynamic response of the sensor has been performed at the flow rate of 500 mL/min while the volume of the cell is about 157 mL. In Fig. 7(a), the rise time (10-90 %) and the fall time (90-10 %) are 16 s and 14 s, respectively. Fig. 7(b) shows the measured value of WMS-2*f*/1*f* signals versus the time at different concentration, and each sample was recorded for 40 s. The results demonstrate the excellent stability and precision of the sensor.

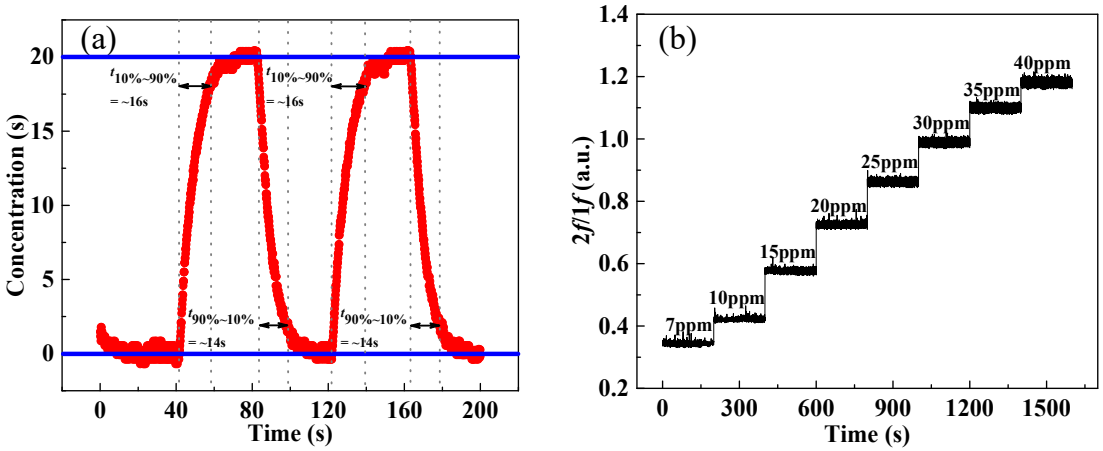

Fig.7 (a) Response time by varying the CH_4 concentration between 0 and 20 ppm; (b) measured WMS-2*f*/1*f* CH_4 signals at different concentrations.

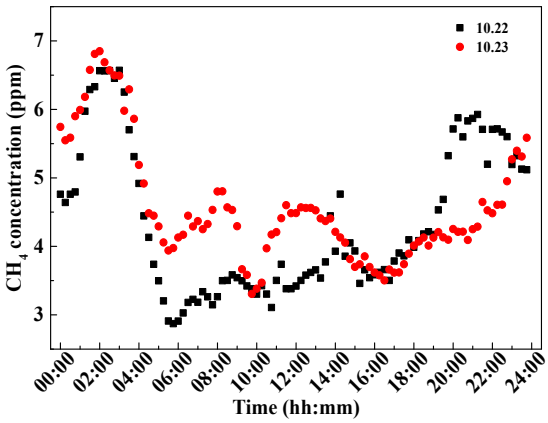

Fig. 8. Measured CH_4 concentrations in atmosphere variation on 2019-10-22 and 2019-10-23.

By real-time and in-situ measurement of CH_4 in ambient air for two days, the performance of the developed CH_4 sensor was validated. The test was conducted on the campus of the Taiyuan University of Science and Technology. It is a mixed-use area with woods, apartments and nearby the Xizhonghuan Road with heavy traffic especially during rush hours. The temporal resolution of the sensor is determined by the scanning frequency of the diode laser (2 s) and the interval of gas extracted into the multi-pass cell (~20 s) which is usually shorter than the time to reach equilibrium of gases. Therefore, the time interval between the measurement and the process of extracting gas into the multi-pass cell does not affect the real-time measurement. During the measurement, a dryer and a particle filter were placed before the inlet of the multi-pass cell to remove humidity and aerosols. The sensor operated continuously during the measurement. The concentrations of ambient CH_4 are shown in Fig. 8, while the data were captured at 0.5 Hz and averaged over 8 laser scans. The results of consecutive measurements in two days indicate the same CH_4 concentration variation trends. The highest concentration of CH_4 occurs at ~2am and the

lowest concentration appears after 5am on both days. Moreover, the CH_4 concentration is higher during the night than at daytime. The photochemical removal of CH_4 from the atmosphere is very slow, leading to an atmospheric lifetime of CH_4 of more than 10 years. Therefore, the variation in the CH_4 concentrations during the day are possibly due to increased mixing of local CH_4 sources after sunrise (6:40 am) while the increase in concentration after sunset (5:40 pm) is due to a decreased boundary layer height.

Conclusions

A portable optical sensor for trace gas quantification with a toroidal cell based on near infrared TDLAS is reported. The 8.35 m optical path length is realized with 84 reflections in two layers in a toroidal cell with an aspheric surface. The WMS-2*f*/1*f* calibration free method is employed to derive the concentration of the absorbing gas. The laser driver is implemented in a home-made electronic system. The minimum achieved detection limit of CH_4 was 22 ppb with an integration time of 57.8 s. To validate the performance of the sensor, we continuously monitored the concentration of CH_4 in ambient air for two days using a DFB laser emitting at 1.653 μm. The results indicate that the sensor is appropriate for monitoring trace gas.

Acknowledgement

The work presented in this paper was supported by National Natural Science Foundation of China (U1810129, 52076145, 11904252 & 42077201), State Key Laboratory of Applied Optics (SKLAO-201902), Transformation of Scientific and Technological Achievements Fund of Shanxi Province (201904D131025), Excellent Youth Academic Leader in Higher Education of Shanxi Province (2018), Key Research and Development Program of Shanxi Province of China (201803D31077, 201803D121090), Shanxi "1331 Project" Key Innovative Research Team (1331KIRT), Natural Science Foundation of Shanxi Province (201801D221017) and Fund for Shanxi Key Subjects Construction.

References

1. Heinrich, K.; Fritsch, T.; Hering, P.; Mürtz, M., Infrared laser-spectroscopic analysis of ^{14}NO and ^{15}NO in human breath. *Applied Physics B* **2009,** *95* (2), 281-286.
2. Meyer, P. L.; Sigrist, M. W., Atmospheric pollution monitoring using CO_2-laser photoacoustic spectroscopy and other techniques. *Review of Scientific Instruments* **1990,** *61* (7), 1779-1807.
3. Wang, M.; Zhang, Y.; Liu, J.; Liu, W.; Kan, R.; Wang, T.; Chen, D.; Chen, J.; Wang, X.; Xia, H., Applications of a tunable diode laser absorption spectrometer in monitoring greenhouse gases. *Chinese Optics Letters* **2006,** *4* (6), 363-365.
4. Hirschmann, C. B.; Sinisalo, S.; Uotila, J.; Ojala, S.; Keiski, R. L., Trace gas detection of benzene, toluene, p-, m- and o-xylene with a compact measurement system using cantilever enhanced photoacoustic spectroscopy and optical parametric oscillator. *Vibrational Spectroscopy* **2013,** *68*, 170-176.
5. Loftfield, N.; Flessa, H.; Augustin, J.; Beese, F., Automated Gas Chromatographic System for Rapid Analysis of the Atmospheric Trace Gases Methane, Carbon Dioxide, and Nitrous Oxide. .*Journal of Environmental Quality* **1997,** *26*, 560-564.
6. Maity, S.; Kaiser, R. I.; Jones, B. M., Formation of Ketene (H_2CCO) in Interstellar Analogous Methane (CH_4)-Carbon Monoxide (CO) ICES: A Combined Ftir and Reflectron Time-of-Flight Mass Spectroscopic Study. *The Astrophysical Journal* **2014,** *789* (1).
7. Tanaka, T.; Miyamoto, Y.; Morino, I.; Machida, T.; Nagahama, T.; Sawa, Y.; Matsueda, H.; Wunch, D.; Kawakami, S.; Uchino, O., Aircraft measurements of carbon dioxide and methane for the calibration of ground-based high-resolution Fourier Transform Spectrometers and a comparison to GOSAT data measured over Tsukuba and Moshiri. *Atmospheric Measurement Techniques* **2012,** *5* (8), 2003-2012.
8. Pogany, A.; Wagner, S.; Werhahn, O.; Ebert, V., Development and metrological characterization of a tunable diode laser absorption spectroscopy (TDLAS) spectrometer for simultaneous absolute measurement of carbon dioxide and water vapor. *Appl Spectrosc* **2015,** *69* (2), 257-268.
9. Zellweger, C.; Steinbacher, M.; Buchmann, B., Evaluation of new laser spectrometer techniques for in-situ carbon monoxide measurements. *Atmospheric Measurement Techniques* **2012,** *5*, 2555-2567.
10. Dong, L.; Tittel, F. K.; Li, C.; Sanchez, N. P.; Wu, H.; Zheng, C.; Yu, Y.; Sampaolo, A.; Griffin, R. J., Compact TDLAS based sensor design using interband cascade lasers for mid-IR trace gas sensing. *Optics Express* **2016,** *24* (6), A528-A535.
11. F.G. Wienhold, H. F.; Hoor, P.; Wagner, V.; Königstedt, R.; Harris, G. W.; Anders, J.; R.Grisar; Knothe, M.; Riedel, W. J.; Lübken, F.-J.; Schilling, T., TRISTAR–atracer in situ TDLAS for atmospheric research. *Applied Physics B* **1998,** *67*, 411-417.
12. Yang, S.; Talbot, R.; Frish, M.; Golston, L.; Aubut, N.; Zondlo, M.; Gretencord, C.; McSpiritt, J., Natural Gas Fugitive Leak Detection Using an Unmanned Aerial Vehicle: Measurement System Description and Mass Balance Approach. *Atmosphere* **2018,** *9* (10).
13. Bennetts, V. M. H.; Lilienthal, A. J.; Khaliq, A. A.; Ses´e, V. ı. P.; Trincavelli, M., Towards Real-World Gas Distribution Mapping and Leak Localization Using a Mobile Robot with 3D and Remote Gas Sensing Capabilities. *IEEE International Conference on Robotics and Automation* **2013**, 2335-2340.
14. White, J. U., Long Optical Paths of Large Aperture. *Journal of the Optical Society of America* **1942,** *32*, 285-288.
15. Pilston, R. G.; John U. White, A Long Path Gas Absorption Cell. *Journal of the Optical Society of America* **1954,** *44*, 572-573.
16. Herriott, D.; Kogelnik, H.; Kompfner, R., D. Herriott, H. Kogelnik, and R. Kompfner. *Applied Optics* **1964,** *3*, 523-526.
17. Guo, X.; Zheng, F.; Yang, X.; Li, N.; Qiu, X.; Wei, J.; Hea, Q.; Li, C., A portable sensor for in-situ measurement of ammonia based on near-infrared laser absorption spectroscopy. *Optics and Lasers in Engineering* **2019,** *115*, 243-248.
18. Li, C.; Shao, L.; Meng, H.; Wei, J.; Qiu, X.; He, Q.; Ma, W.; Deng, L.; Chen, Y., High-speed multi-pass tunable diode laser absorption spectrometer based on frequency-modulation spectroscopy. *Optics Express* **2018,** *26* (22), 29330-29339.
19. Chernin, S. M.; Barskaya, E. G., Optical multipass matrix systems. *Applied Optics* **1991,** *30*, 51-58.
20. Tuzson, B.; Mangold, M.; Looser, H.; Manninen, A.; Emmenegger, L., Compact multipass optical cell for laser spectroscopy. *Optics Letters* **2013,** *38* (3), 257-259.

21. Jouy, P.; Mangold, M.; Tuzson, B.; Emmenegger, L.; Chang, Y. C.; Hvozdara, L.; Herzig, H. P.; Wagli, P.; Homsy, A.; de Rooij, N. F.; Wirthmueller, A.; Hofstetter, D.; Looser, H.; Faist, J., Mid-infrared spectroscopy for gases and liquids based on quantum cascade technologies. *Analyst* **2014,** *139* (9), 2039-46.
22. Chang, H.; Feng, S.; Qiu, X.; He, X.; He, Q.; Yang, X.; Ma, W.; Kan, R.; Fittschen, C.; Li, C., Implementation of the toroidal absorption cell with multi-layer patterns by a single ring surface. *Optics letters* **2020**, 5897-5900.
23. Kluczynski, P.; Gustafsson, J.; Lindberg, A. M.; Axner, O., Wavelength modulation absorption spectrometry - an extensive scrutiny of the generation of signals. *Spectrochimica Acta Part B: Atomic Spectroscopy* **2001,** *56(8)*, 1277-1354.
24. Rieker, G. B.; Jeffries, J. B.; Hanson, R. K., Calibration-free wavelength-modulation spectroscopy for measurements of gas temperature and concentration in harsh environments. *Applied Optics* **2009,** *48(29)*, 5546-5560.
25. Wang, G.; Mei, J.; Tian, X.; Liu, K.; Tan, T.; Chen, W.; Gao, X., Laser frequency locking and intensity normalization in wavelength modulation spectroscopy for sensitive gas sensing. *Optics Express* **2019,** *27* (4), 4878-4885.
26. Qu, Z.; Ghorbani, R.; Valiev, D.; Schmidt, F. M., Calibration-free scanned wavelength modulation spectroscopy--application to H(2)O and temperature sensing in flames. *Optics Express* **2015,** *23* (12), 16492-9.
27. Willis, J. L., GHG Methodologies for Sewer CH_4, Methanol-Use CO_2, and Biogas-Combustion CH_4 and their Significance for Centralized Wastewater Treatment. **2017**.
28. Saunois, M.; Bousquet, P.; Poulter, B.; Peregon, A.; Ciais, P.; Canadell, J. G.; Dlugokencky, E. J.; Etiope, G.; Bastviken, D.; Houweling, S.; Janssens-Maenhout, G.; Tubiello, F. N.; Castaldi, S.; Jackson, R. B.; Alexe, M.; Arora, V. K.; Beerling, D. J.; Bergamaschi, P.; Blake, D. R.; Brailsford, G.; Brovkin, V.; Bruhwiler, L.; Crevoisier, C.; Crill, P.; Covey, K.; Curry, C.; Frankenberg, C.; Gedney, N.; Höglund-Isaksson, L.; Ishizawa, M.; Ito, A.; Joos, F.; Kim, H.-S.; Kleinen, T.; Krummel, P.; Lamarque, J.-F.; Langenfelds, R.; Locatelli, R.; Machida, T.; Maksyutov, S.; McDonald, K. C.; Marshall, J.; Melton, J. R.; Morino, I.; Naik, V.; O'Doherty, S.; Parmentier, F.-J. W.; Patra, P. K.; Peng, C.; Peng, S.; Peters, G. P.; Pison, I.; Prigent, C.; Prinn, R.; Ramonet, M.; Riley, W. J.; Saito, M.; Santini, M.; Schroeder, R.; Simpson, I. J.; Spahni, R.; Steele, P.; Takizawa, A.; Thornton, B. F.; Tian, H.; Tohjima, Y.; Viovy, N.; Voulgarakis, A.; van Weele, M.; van der Werf, G. R.; Weiss, R.; Wiedinmyer, C.; Wilton, D. J.; Wiltshire, A.; Worthy, D.; Wunch, D.; Xu, X.; Yoshida, Y.; Zhang, B.; Zhang, Z.; Zhu, Q., The global methane budget 2000–2012. *Earth System Science Data* **2016,** *8* (2), 697-751.
29. Vojtisek-Lom, M.; Beranek, V.; Klir, V.; Jindra, P.; Pechout, M.; Vorisek, T., On-road and laboratory emissions of NO, NO2, NH3, N2O and CH4 from late-model EU light utility vehicles: Comparison of diesel and CNG. *Science of the Total Environment* **2018,** *616-617*, 774-784.
30. Qu, S.; Wang, M.; Li, N., Mid-Infrared Trace CH4 Detector Based on TDLAS-WMS. *Guang Pu Xue Yu Guang Pu Fen Xi* **2016,** *36* (10), 3174-3178.
31. Dong, L.; Li, C.; Sanchez, N. P.; Gluszek, A. K.; Griffin, R. J.; Tittel, F. K., Compact CH_4 sensor system based on a continuous-wave, low power consumption, room temperature interband cascade laser. *Applied Physics Letters* **2016,** *108* (1).
32. Liu, K.; Wang, L.; Tan, T.; Wang, G.; Zhang, W.; Chen, W.; Gao, X., Highly sensitive detection of methane by near-infrared laser absorption spectroscopy using a compact dense-pattern multipass cell. *Sensors and Actuators B: Chemical* **2015,** *220*, 1000-1005.
33. Cui, R.; Dong, L.; Wu, H.; Ma, W.; Xiao, L.; Jia, S.; Chen, W.; Tittel, F. K., Three-Dimensional Printed Miniature Fiber-Coupled Multipass Cells with Dense Spot Patterns for ppb-Level Methane Detection Using a Near-IR Diode Laser. *Analytical Chemistry* **2020**.
34. Salati, S. H.; Khorsandi, A., Apodized 2f/1f wavelength modulation spectroscopy method for calibration-free trace detection of carbon monoxide in the near-infrared region: theory and experiment. *Applied Physics B* **2013,** *116* (3), 521-531.
35. Topfer, T.; Petrov, K. P.; Mine, Y.; Jundt, D.; Curl, R. F.; Tittel, F. K., Room-temperature mid-infrared laser sensor for trace gas detection. *Applied Optics* **1997,** *36(30)*, 8042-8049.
36. Gordon, I. E.; Rothman, L. S.; Hill, C.; Kochanov, R. V.; Tan, Y.; Bernath, P. F.; Birk, M.; Boudon, V.; Campargue, A.; Chance, K., The HITRAN2016 molecular spectroscopic database. *Journal of Quantitative Spectroscopy and Radiative Transfer* **2017,** *203*, 3-69.
37. Sur, R.; Sun, K.; Jeffries, J. B.; Hanson, R. K., Multi-species laser absorption sensors for in situ monitoring of syngas composition. *Applied Physics B* **2013,** *115* (1), 9-24.
38. Ste´ phane Schilt, L. T. v., and Philippe Robert, Wavelength modulation spectroscopy: combined frequency and intensity laser modulation. *Applied Optics* **2003,** *42(33)*, 6728-6738.

Table of Content Graphic

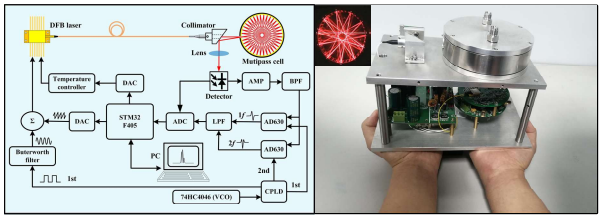

For Table of Contents Only